Ecological Informatics 87 (2025) 103075

Contents lists available at ScienceDirect

Ecological Informatics

journal homepage: www.elsevier.com/locate/ecolinf

Rice cropping sequence mapping in the tropical monsoon zone via agronomic knowledge graphs integrating phenology and remote sensing

Hongzhang Nie [a,b], Yingchen Lin [a], Wenfei Luo [a], Guilin Liu [a,*]

[a] School of Geography, South China Normal University, Guangzhou, China
[b] Faculty of Geographical Science, Beijing Normal University, Beijing, China

A R T I C L E I N F O

Keywords:
Agronomic knowledge graphs
Phenology events
Random forest
Pixel- and object-based classification

A B S T R A C T

Rice cropping sequence mapping via multitemporal remote sensing and agronomic techniques provides critical geoinformatics for agroecosystem modeling. The East Asian tropical monsoon region is an important rice-growing area, and the regional food security depends on efficient rice mapping. Frequent cloud cover during the rainy season leads to insufficient available optical remote sensing images that cover the growth stages of rice, which renders remote sensing-derived rice identification difficult. Thus, we proposed a simple and efficient strategy from an agronomic knowledge graph perspective in which specific phenological events of rice and Landsat/Sentinel-2 time series were employed to extract different rice cropping sequences on the Leizhou Peninsula (China). Then, a control group and five experimental groups were established by integrating spectral features via pixel- and object-based random forest (RF) algorithms. The results revealed that five key phenological events could be obtained for rice cropping sequence identification in the study area. The overall accuracy of the pixel-based classification results ranged from 83.48 % to 92.49 %, whereas that of the object-based classification results ranged from 84.98 % to 92.80 %. These findings indicate that efficient rice cultivation mapping via optical remote sensing data requires the selection of specific time windows corresponding to phenological events to benefit rice cultivation monitoring and regional agroecosystem sustainability.

1. Introduction

Rice is one of the most important food crops in the world, as rice feeds nearly half of the global population, and with population growth, the demand for food is increasing (Kuenzer and Knauer, 2013; Shi et al., 2024; Zhao et al., 2021). At present, environmental pollution and the depletion of natural resources are problems associated with crop cultivation (Meng et al., 2023). Mapping rice cultivation areas is important for predicting grain yields (Wu et al., 2021), assessing food security and improving agricultural and ecological policy planning at the regional, national, and global scales (Sah et al., 2023). Remote sensing is an essential technology for monitoring rice cultivation (Kuenzer and Knauer, 2013) and supports precision farming by guiding field management activities, such as sowing, irrigation and fertilization (Meng et al., 2015). Machine learning methods have been widely applied in crop classification (Fu et al., 2023), and common methods, including the support vector machine (SVM) (Yan et al., 2021) and random forest (RF) (Li et al., 2021a) methods, have achieved excellent accuracy in previous studies (de Azevedo et al., 2023; Pelletier et al., 2016). Characterizing the time series variations in agronomic traits and vegetation indices during the growing season is the key to constructing a remote sensing monitoring model (Duarte et al., 2014; Zhao et al., 2022). Common methods for extracting rice characteristics usually entail the use of as many features as possible to increase the classification accuracy or involve the selection of remote sensing features (such as spectral, index and textural features) for establishing and evaluating feature combinations (Liu et al., 2022). However, useful information occurs in the low-dimensional feature space (Hu et al., 2017). The increase in features may even cause a decline in the classification accuracy with a limited amount of training data (Hughes, 1968). In addition, surface reflectance and vegetation indices from remote sensing data have been used indiscriminately for mapping various crops (Ferchichi et al., 2022). However, employing unique phenological features of crops can yield a better feature space than employing common vegetation indices can (Zhang et al., 2020a), and such features have been integrated into remote sensing modeling and classification of tea plantations (Kang et al., 2023), grasses (Rojo et al., 2022) and ecosystem dynamics (Caparros-Santiago et al., 2023), with a high overall accuracy (OA) and fine-scale

* Corresponding author.
E-mail addresses: liuguilin@m.scnu.edu.cn, guilinshiwo@163.com (G. Liu).

https://doi.org/10.1016/j.ecoinf.2025.103075
Received 9 May 2024; Received in revised form 9 February 2025; Accepted 13 February 2025
Available online 14 February 2025

mapping results.

Crop phenology events and traits can aid in remote sensing for distinguishing different crop types and cropping sequences (Blickensdörfer et al., 2022; Duarte et al., 2014; Singha and Sarmah, 2019; Wardlow and Egbert, 2008). Cropping sequences describe the arrangements used in crop succession planting for the same cropland parcel, including continuous plantings of the same crop and diverse crop rotations (Leteinturier et al., 2006; Steinmann and Dobers, 2013). The commonly applied phenology parameters derived from remote sensing data include the start of the season (SOS), end of the season (EOS) (de Beurs and Henebry, 2010), maximum normalized difference vegetation index (NDVI) (Reed et al., 1994), green-up stage, maturity, senescence, dormancy (Duarte et al., 2014; Zhang et al., 2003), and time of the maximum recoded during the growth period (Araya et al., 2018). As one of the most widely adopted vegetation indices, the NDVI has been used to obtain crop phenological information (Araya et al., 2018), for which different phenological methods have been proposed in rice cultivation mapping: (1) To introduce phenological features into remote sensing classification, for example, Zhang and Lin (2019) used five phenology parameters based on fitted NDVI curves as feature bands to map rice; furthermore, (2) remote sensing data for key phenological stages have been incorporated for crop classification. For instance, Li et al. (2016) noted two key phenological stages of rice, proposed a renormalized version of the NDVI, and employed Landsat Thematic Mapper (TM)/ Enhanced Thematic Mapper Plus (ETM+) images from early August and early October to classify these stages, resulting in an OA value of 98.9 %. Zhang et al. (2020a) applied classification and regression tree (CART), SVM and RF models to conduct classification on the basis of the features of eight-temporal-phase Sentinel-2 images, thereby achieving an OA value of 97.85 %. In recent years, pixel-based classification has become a common method for crop identification (Pluto-Kossakowska, 2021). Notably, Ni et al. (2021) developed a pixel-based phenological feature composite method and inputted the derived features into a classifier to obtain classification results. Considering the salt-and-pepper effect in pixel-based classification, the object-based approach has been more frequently employed for crop identification and has provided greater classification accuracy (Gao and Mas, 2008; Jiao et al., 2022). By integrating the geometric features of cropland objects from Gaofen (GF)-2 high-resolution images and spectral–temporal features from Sentinel-2 time series, Chen and Liu (2024) mapped crop types on the basis of phenology knowledge, with an OA value of 99.64 %, thus revealing the potential for crop mapping under spatially heterogeneous cropland conditions.

Cloud coverage is a major obstacle in capturing adequate optical remote sensing data in the tropical monsoon zone (Laborde et al., 2017). During the rainy season, the frequent occurrence of cloud coverage renders it difficult to obtain sufficient cloud-free images at the rice phenological stages, which poses challenges for effectively using vegetation indices derived from satellite optical images to map rice cropping sequences (Jiang et al., 2021). To solve this problem, high-temporal-resolution and high-spatial-resolution (daily 30-m) data have been generated via spatiotemporal fusion models (such as the spatial and temporal adaptive reflection fusion model (STARFM)) (Gao et al., 2006). The abovementioned methods exhibit limitations; for example, the spatiotemporal model performance is significantly affected by spatiotemporal variations in landscapes. Notably, the model prediction accuracy cannot be enhanced, even with a higher computational cost (Chen et al., 2015). However, the rice mapping method is efficient and easy to implement (Mosleh et al., 2015). Thus, a simple and efficient strategy that relies on specific phenological events of rice and corresponding time series remote sensing data can be employed for efficient crop classification, which can benefit yield prediction and agricultural policy-making efforts (Yang et al., 2024; Zhang and Lin, 2019).

The Leizhou Peninsula of China is an important agricultural area where various cropping sequences are implemented. Notably, rice is grown during the rainy season, and fruits and vegetables are grown during the dry season. In this study, we first established and analyzed an agronomic remote sensing knowledge graph for cropping sequence identification in the tropical monsoon zone and then hypothesized that the early-season rice harvesting period and the late-season rice harvesting period are two key phenological events for identifying cropping sequences. To test this hypothesis, we established a control group and five experimental groups by integrating remote sensing bands and NDVI features and applying pixel- and object-based RF classification algorithms (Breiman, 2001). Specifically, this study aimed to (1) analyze agronomic remote sensing knowledge graphs for cropping sequence identification and emphasize their importance; (2) construct image feature subsets to evaluate key phenological events for classification; and (3) evaluate the optimization of object-based classification results over pixel-based results in fragmented agricultural areas.

2. Theoretical framework

As shown in Fig. 1, we established a theoretical framework for analyzing agronomic remote sensing knowledge graphs, which constitutes the basis for cropping sequence identification in the tropical monsoon zone. Data from multisource remote sensing satellite images (e.g., Landsat and Sentinel), crop planting information, agronomic practices, and policy information are fundamental for classification mapping. These massive data must be preprocessed, which includes data filtering, image merging after cloud masking, image segmentation and identification of field objects. The process-stage model (Zhang et al., 2022) of crop growth is the core of the entire knowledge graph. The process refers to the continuous process of crop growth, including rice sowing, seedling, transplanting, tillering to stem elongation, panicle initiation to heading, filling, maturity and winter planting. The stage may be divided into two categories: (1) phenological events, which are supported by existing agronomic knowledge, farm management patterns and agronomic policies; and (2) remote sensing time windows corresponding to these events. In this study, an ontology was established comprising concepts (e.g., rice, phenology), attributes (e.g., surface reflection and vegetation indices), and farmland entities (e.g., fields and field edges). Notably, the intrayear variations in vegetation indices reflect the crop growth process. The use of images for different remote sensing time windows (stages) facilitates the extraction of features such as surface reflectance and vegetation indices. Feature mining is performed on the basis of the key phenological events (stages). Thus, information extraction can be achieved via machine learning (e.g., the RF) or deep learning (e.g., convolutional neural networks). In general, the construction of agronomic knowledge graphs focuses on the division of stages, which involves first extracting key phenological events on the basis of agronomic knowledge and then dividing time windows. The accuracy of stage division in agronomic knowledge graphs affects feature space construction and directly impacts the crop classification accuracy. Eventually, remote sensing knowledge graphs of agricultural management policy can be used for managing agricultural natural resources and optimizing agricultural policies, thus realizing precision agricultural management.

3. Case study: rice cropping sequence mapping in the tropical monsoon zone of China

3.1. Study area and data

We selected an area of 5.82×7.14 km^2 in the central part of the Leizhou Peninsula in China as the study area (Fig. 2). The average annual temperature ranges from 23 to 24 °C, and the annual precipitation ranges from 1400 to 1700 mm and is affected by the tropical monsoon climate. The study area is suitable for growing rice during the rainy season because of the flat cropland, fertile soil, and sufficient water supply, and it is suitable for growing winter crops, such as greenhouse watermelon, during the dry season (Yang, 2018).

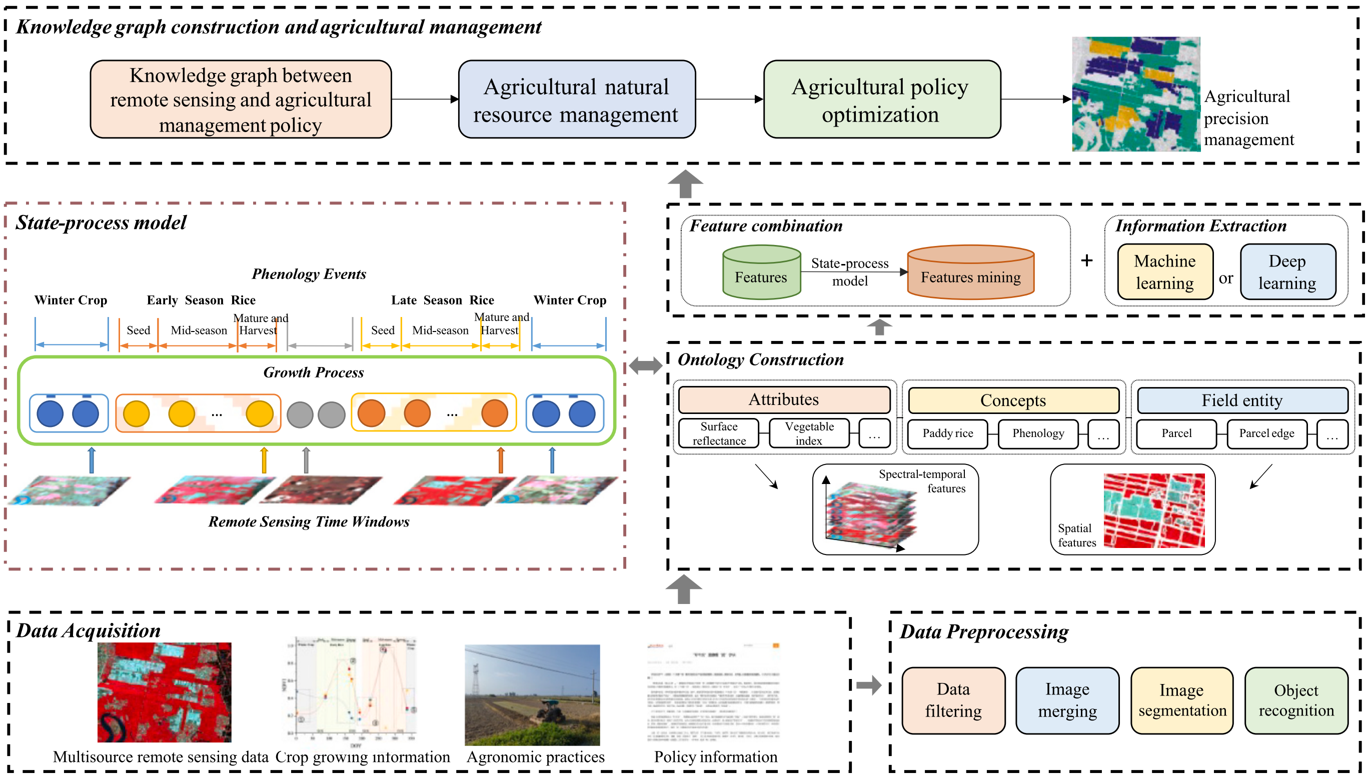

Fig. 1. Framework of agronomic remote sensing knowledge graph construction for cropping sequence identification. The policy information image was acquired from https://www.gdzjdaily.com.cn/p/2830978.html (accessed on 10 February 2023).

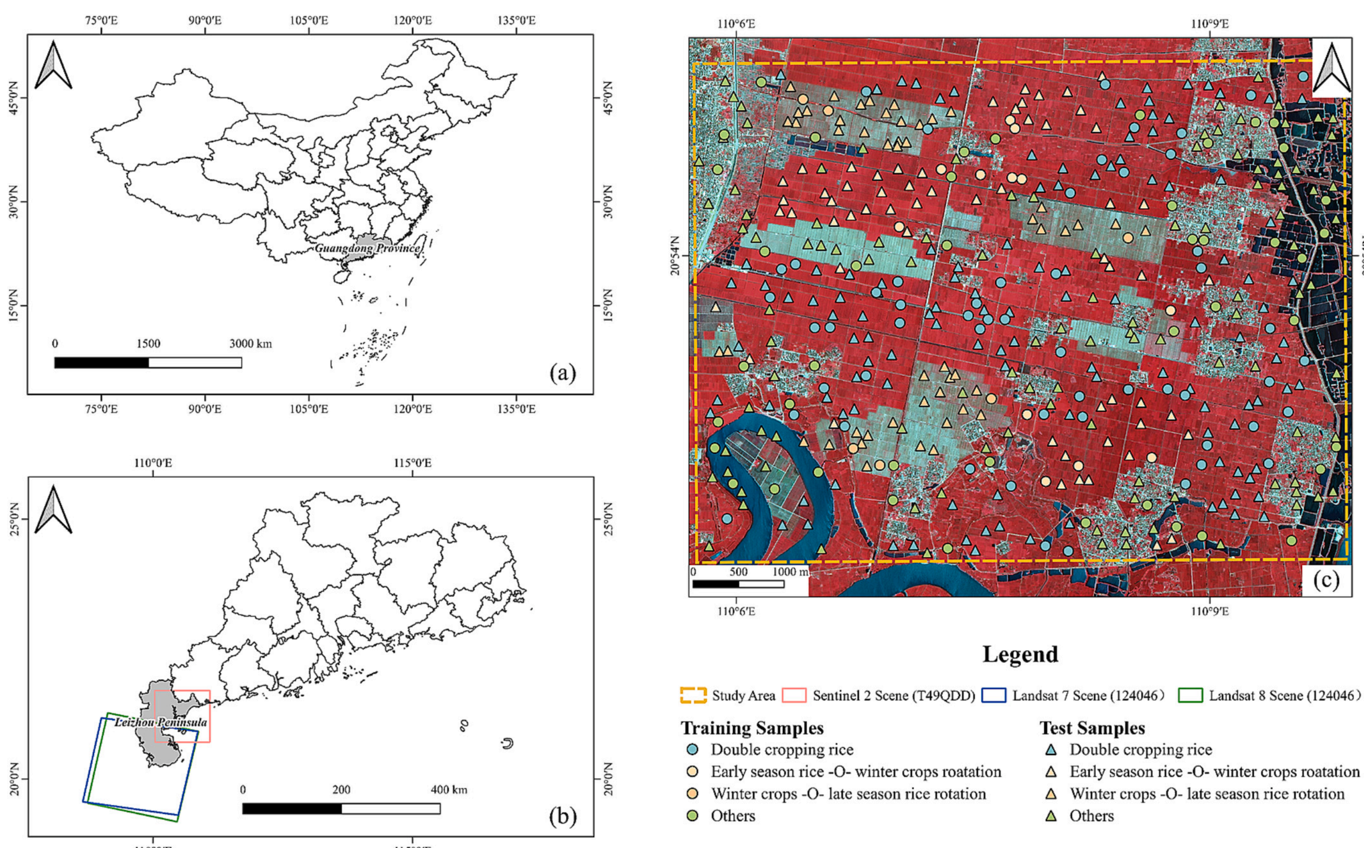

Fig. 2. Location of the study area: (a) Location of Guangdong Province in China; (b) location of the Leizhou Peninsula in Guangdong Province and the area covered by satellite images; (c) boundary of the study area and distribution of the training and validation points.

Throughout the year, the main cropping sequences are double-cropping rice (DCR), early-season rice–O–winter crop rotation (EOWR), and winter crop–O–late-season rice rotation (WOLR). Notably, O denotes the fallow period between the winter crop and rice rotations. According to interviews with farmers and local news, early-season rice is generally sown in March and harvested from mid-June to late June, whereas late-season rice is generally sown from late July–early August and harvested in November.

Satellites such as the GF satellites (Chinese high-resolution Earth imaging satellites) provide data with a very high spatial resolution, thus offering a direct solution for crop mapping in smallholder agricultural areas (Zhang et al., 2020b). We obtained the GF-1 product from the Guangdong High-Resolution Earth Observation System Guangdong Data and Application Center (https://www.gdgf.gd.gov.cn/). In particular, the GF-1 satellite was launched on April 26, 2013, and carries two high-resolution 2-m panchromatic and 8-m multispectral cameras (Wu et al., 2017). In this study, the obtained GF data provided parcel spatial information and were used for segmentation in object-based classification. We used Environment for Visualizing Images (ENVI) software (https://envi.geoscene.cn/) to implement radiometric and geometric corrections of the GF-1 high-resolution remote sensing data. We also obtained Landsat-7 and Landsat-8 Level 2 products from the U.S. Geological Survey (USGS, https://earthexplorer.usgs.gov/) and Sentinel-2 L2A products from the European Space Agency (ESA). We then applied the nearest neighbor method (Shang et al., 2022) to resample the Sentinel-2 remote sensing data to a 30-m resolution to ensure land cover identification (Jombo and Adelabu, 2023). We also filled any unscanned pixels in the Landsat-7 images according to the method of Li et al. (2021b). In addition, owing to the occurrence of cloud coverage in the Landsat-8 images acquired on July 12 and August 13, 2021, they were subjected to cloud masking and fused via the Google Earth Engine (GEE) (Gorelick et al., 2017). Finally, the vectorized boundary of the study area was employed for clipping the abovementioned images to match the study area (Table 1).

We collected 42 crop samples in the field on February 10 and 11, 2023 (Fig. 3). On the basis of the abovementioned crop samples and interviews with farmers, we identified cropping sequences in the corresponding objects in 2021. Moreover, features corresponding to the crop samples, including color, shape, size, and texture, were learned from the Landsat-7/8 and Sentinel-2 images acquired on different dates. The temporal features of the crop samples were also learned from NDVI multitemporal profiles generated from the Landsat-7/8 and Sentinel-2 images. To expand the samples, 400 sample points were randomly created in ArcGIS software with a minimum allowable distance of 100 m. We interpreted the class of each random point on the basis of learned prior knowledge. A total of 13 samples were excluded because of their locations at both object edges and in mixed pixels. This mixed-pixel problem might cause errors in supervised classification or accuracy assessment. Finally, the remaining 387 sample points were separated into training and validation samples, which accounted for 30 % and 70 %, respectively, of the total sample points (Li et al., 2021b). A total of 4 DCR test samples, 19 EOWR test samples, 35 WOLR test samples and 5 other test samples were added to balance the number of samples of each class (Table 2). Considering the phenology of rice, June and September are possible months for distinguishing between the DCR, EOWR, and WOLR sequences because both early- and late-season rice mature in these months, respectively, which can be easily observed in the field and via satellite. In addition, February and December are possible months for distinguishing between the EOWR and WOLR sequences, since the former is the winter crop planting period for WOLR, whereas the latter is the winter crop planting period for EOWR.

Table 1
Remote sensing image data. Specifically, GF-1 images were pansharpened from 2-m panchromatic images and 8-m multispectral scanning images.

Remote sensing satellites	Acquisition date	Resolution	Coordinate system	Notes
Landsat-8	01-01-2021	30 m	WGS84[a]	
Landsat-7	30-03-2021	30 m	UTM[b] zone	Gaps filled
GF-1	15-05-2021	2 m, 8 m	49 N	
Landsat-8	10-06-2021	30 m		
Landsat-7	18-06-2021	30 m		Gaps filled
Landsat-8	12-07-2021	30 m		Less cloudy, clouds removed and combined
	13-08-2021	30 m		
Sentinel-2	29-09-2021	10 m		
Landsat-8	30-09-2021	30 m		Less cloudy
Landsat-8	03-12-2021	30 m		

[a] WGS84: World Geodetic System 1984.
[b] UTM: Universal Transverse Mercator.

3.2. Methods

Fig. 4 shows the technical flow chart of this study. First, the obtained remote sensing images and the sample points were preprocessed on the GEE platform and in ENVI software. The images and corresponding NDVI images were employed as features. The feature space was constructed by combining these images into feature subsets according to the time series and phenological events. Second, several classification processes were conducted via the feature subsets, with pixel-scale classification according to the RF classifier in ENVI software and object-scale classification according to the RF classifier in eCognition software (Trimble Germany GmbH, 2014). Finally, the OA, producer accuracy (PA), user accuracy (UA), and kappa coefficient were assessed via the confusion matrix (Congalton, 1991) in ENVI and eCognition software.

3.2.1. Experimental design

Time series remote sensing images can capture cropping sequences that describe the arrangement of crop succession within the same cropland object, including continuous plantings of the same crop and diverse rotations (Leteinturier et al., 2006; Steinmann and Dobers, 2013). The three main cropping sequences are DCR, EOWR, and WOLR. The winter crop planting period (*I*), early-season rice maturation period (*II*), early-season rice harvesting period (*III*), late-season rice maturation period (*IV*), and winter crop planting period (*V*) are the key phenological events that distinguish these cropping sequences in the study area. Specifically, *I* is the first winter crop planting period or SOS for early-season rice; *II* is the early-season rice maturation period or NDVI peak period; *III* is the EOS for early-season rice harvesting or rice planting; *IV* is the late-season rice maturation period or NDVI peak period; and *V* is the second winter crop planting period or EOS for late-season rice. The NDVI peak period can be used to identify the intensity of the peak vegetative stage, which represents the rice maturation period (Liepa et al., 2024).

On the basis of the abovementioned five key phenological events for identifying cropping sequences, the remote sensing images acquired within the corresponding time windows play a key role in classification. To test the hypothesis that the early-season rice harvesting period (*II*) and the late-season rice harvesting period (*IV*) are two key phenological events for identifying cropping sequences, six feature subsets, including the control group (Ctrl) and the five experimental groups (Exps. 1–5), were combined from the obtained surface reflectance and NDVI features in six bands of each time window (Fig. 5 and Table 3). As shown in Fig. 5, the orange dots indicate cloud-free Landsat-8 satellite images; the green dots indicate cloud-masked and fused Landsat-8 images; and the blue dots indicate cloud-free Sentinel-2 satellite images. For specific features, the surface reflectance features in the six bands were derived from Landsat-8 and Sentinel-2 images.

3.2.2. Cropland object extraction

To extract cropland objects, the vector of the study area was used to divide the GF-1 image, and eCognition software was employed for

Fig. 3. Spatial distribution of the crop samples collected during field work on February 10 and 11, 2023: (a) Winter crop planting; (b) soil solarization after tilling; (c) first soil tilling; (d and e) before the first soil tilling; and (f) first soil tilling.

Table 2
Number of samples in the four categories.

Class	Training samples	Test samples
Double-cropping rice (DCR)	54	116
Early-season rice–O–winter crop rotation (EOWR)	12	60
Winter crop–O–late-season rice rotation (WOLR)	6	49
Others	44	109
Total	116	334

multiresolution segmentation. The estimation of scale parameter (ESP) 2 tool (Drăguţ et al., 2014) was used to estimate the optimal segmentation scale, which can be employed to assess the optimal multiresolution segmentation scale, by automatically calculating the local variance (LV) and the rate of change (ROC). The ROC thresholds of the LV indicate the scales at which the image can be segmented in the most appropriate manner relative to the properties of the data at the scene level (Drăguţ et al., 2010). On the basis of the segmentation results, postclassification was then implemented to modify the vector boundaries of the cropland objects via ArcGIS software. The newly obtained results were then imported into eCognition software for subsequent classification.

3.2.3. Classification and accuracy assessment

We employed an RF classification model to obtain a rice cropping sequence map. The RF algorithm is an integrated classifier comprising multiple decision trees whose predictions are generated on the basis of the majority of the classification results between the trees (Rahmati et al., 2022), which has provided superior performance in remote sensing applications (Avci et al., 2023). Notably, pixel-based RF classification was implemented in ENVI software via the encapsulated ENMAP-BOX v2.1.1 code (van der Linden et al., 2015), whereas object-based RF classification was implemented in eCognition software. The RF algorithm provides two tuning parameters, namely, the number of trees needed to establish an ensemble, which is denoted as Number of Trees, and the minimum number of samples needed to stop splitting, which is denoted as Min Node Samples (Mahlayeye et al., 2024; van der Linden et al., 2015). In the search process, we employed Number of Trees parameter values between 75 and 105 and Min Node Samples parameter values between 5 and 20 at intervals of 5 to obtain the optimal parameters for classification (Tables S1 and S2, respectively). Moreover, OA, PA, UA, and kappa coefficient values were calculated to evaluate the classification accuracy (Belgiu and Csillik, 2018).

3.3. Results

3.3.1. Key phenological events for cropping sequence mapping

In the process-stage model of the agronomic remote sensing knowledge graph, the phenology is the main topic and provides basic information. As shown in Fig. 6, in the NDVI profile of the DCR sequence during the rainy season, there were two peaks (*II* and *IV*) and one valley (*III*) between the early-season rice harvest and late-season rice planting. In the NDVI profile of the EOWR sequence during the rainy season, there was only one peak (*II*) during the first half of the year. In the NDVI profile of the WOLR sequence during the rainy season, there was only one peak (*IV*) during the second half of the year. Therefore, features of the early-season rice maturation period (*II*) and the late-season rice maturation period (*IV*) can be used to distinguish the DCR, EOWR and WOLR sequences.

The dry season corresponds mainly to the winter crop planting period. The NDVI values of the three cropping sequences were relatively low during the dry season, i.e., approximately 0.2–0.5 (Fig. 6). For the winter cropping period during the first half of the year, the NDVI values of the DCR and EOWR sequences were similar and low, whereas the NDVI value of the WOLR sequence was relatively high. During the second half of the winter cropping period, the NDVI values of the DCR and WOLR sequences were similar and low, whereas the NDVI value of the EOWR sequence was relatively high.

In summary, the abovementioned five key phenological events constrain the overall trend in the NDVI profiles of the three cropping

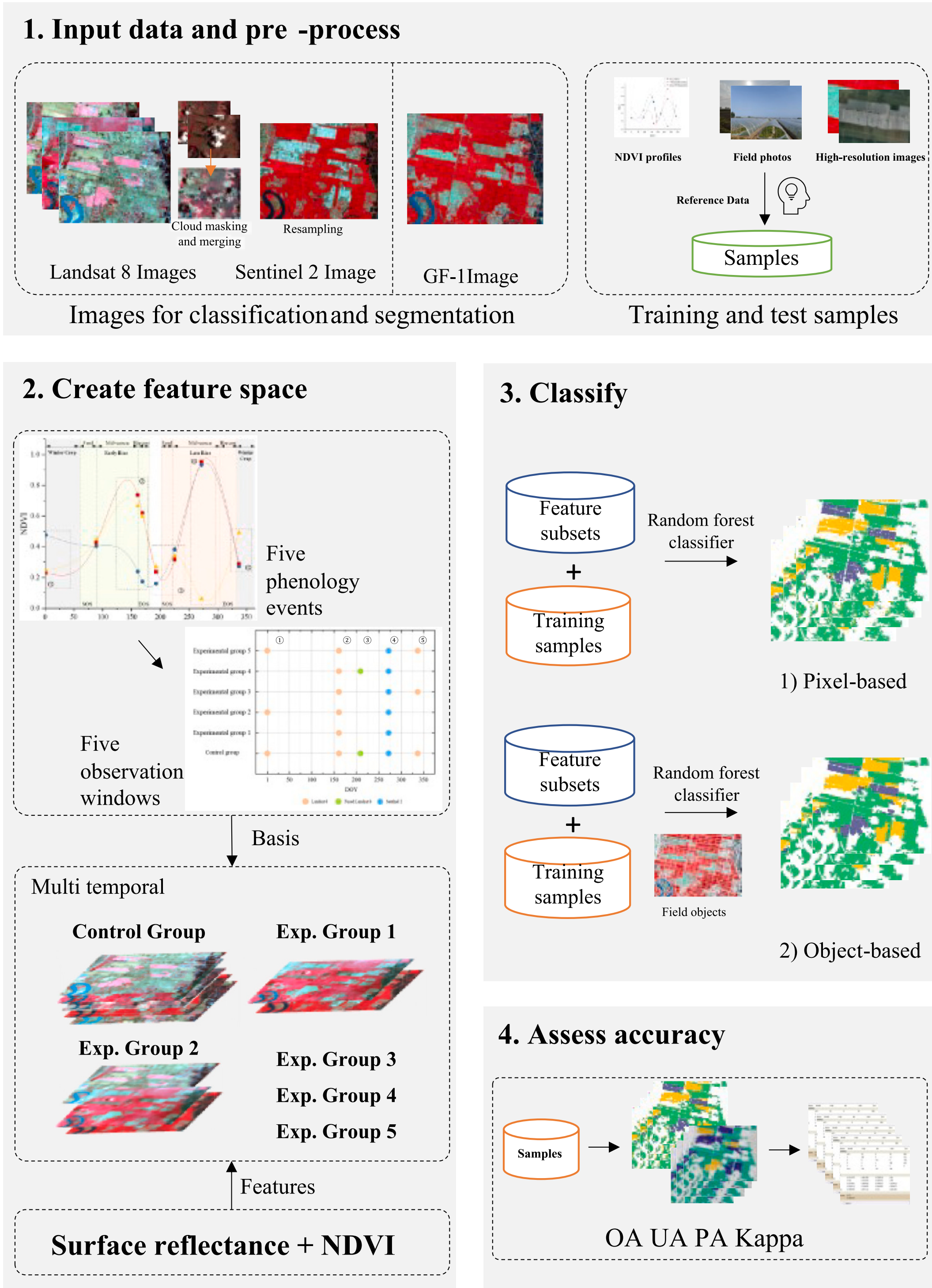

Fig. 4. Flow chart of this study.

sequences and are indicative of the distribution of rice cropping types in the study area.

3.3.2. Cropping sequence mapping results

As indicated in Table 4, the accuracy of the control and experimental groups was generally excellent. The OA values of the RF model ranged from 83.48 % to 92.49 %, and the corresponding kappa coefficient values ranged from 0.769 to 0.895. The highest OA value was obtained in the control group with the features of the five time window images, whereas the lowest OA value was obtained in Exp. 1 with the features of the two time window images. Two key phenology events (*II* and *IV*) were captured in Exp. 1, and these events exhibited considerable accuracy, with the OA and kappa coefficient values of Exp. 1 reaching 83.48 % and 0.769, respectively. However, compared with the results of Ctrl, the OA value of Exp. 5 was 1.2 % lower, indicating that the features of *III* were less important in the classification process.

In addition, object-based RF classification was implemented. As shown in Fig. 7, for scales of 124, 142, and 180, several peaks in the ROC–LV graph indicated optimal scaling parameters. The segmentation performance was better for segmentation scale, shape index and

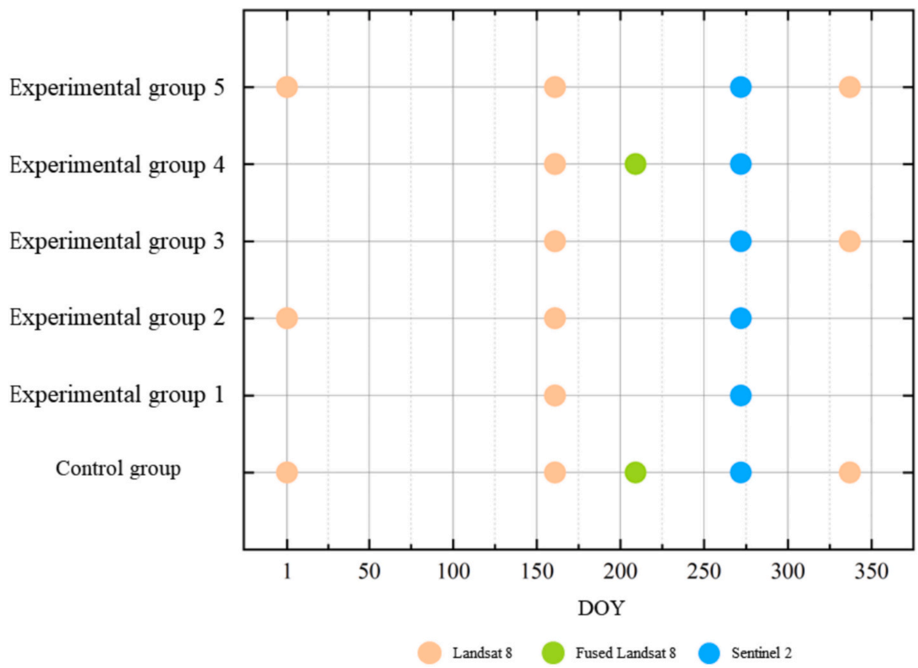

Fig. 5. Patterns of the combined control and experimental groups.

Table 3
Definitions of the control and experimental groups.

Group*	Definition**
Ctrl	This group contains the features of *I*, *II*, *III*, *IV* and *V*.
Exp. 1	This group contains the features of *II* and *IV*.
Exp. 2	This group contains the features of *I*, *II* and *IV*.
Exp. 3	This group contains the features of *II*, *IV* and *V*.
Exp. 4	This group contains the features of *II*, *III* and *IV*.
Exp. 5	This group contains the features of *I*, *II*, *IV* and *V*.

* Ctrl refers to the control group, and Exp. refers to the experimental group.
** *I*, *II*, *III*, *IV* and *V* refer to the winter crop planting period, early-season rice maturation period, early-season rice harvesting period, late-season rice maturation period, and winter crop planting period, respectively.

tightness values of 124, 0.9 and 0.1, respectively. Table 5 provides a summary of the accuracy assessment results for object-based RF classification. Similar to the pixel-based results, Exp. 1 still reached considerable accuracy, with an OA value of 84.98 % and a kappa coefficient value of 0.787. In general, the performance of object-based classification was better than that of pixel-based classification, with OA values ranging from 84.98 % to 92.80 % and corresponding kappa coefficients ranging from 0.787 to 0.900. In object-based classification, the OA value of Exp. 4 increased the most, with a gain of 2.4 %, whereas the OA values of Ctrl and Exp. 5 increased the least, with a gain of 0.31 %.

Fig. 8 shows the pixel- and object-based classification mapping results. In the pixel-based classification results, the control group provided the best spatial detail, followed by Exp. 5, with some object edges identified as EOWR pixels. However, in the results of Exps. 2, 3, and 4, some EOWR pixels were classified into the DCR category. With the salt-and-pepper effect occurring in the pixel-based classification results, the object-based classification results exhibited finer spatial detail. This approach can be used to distinguish between objects and their edges more effectively and overcome the salt-and-pepper effect.

Table 6 provides the areal statistic pixel- and object-based classification results. Among the three cropping sequences, the DCR sequence occupied the largest area, whereas the WOLR sequence occupied the smallest area in the study area. A comparison of the cropping sequence mapping results indicated that the two classification methods also exhibited consistency in terms of the area.

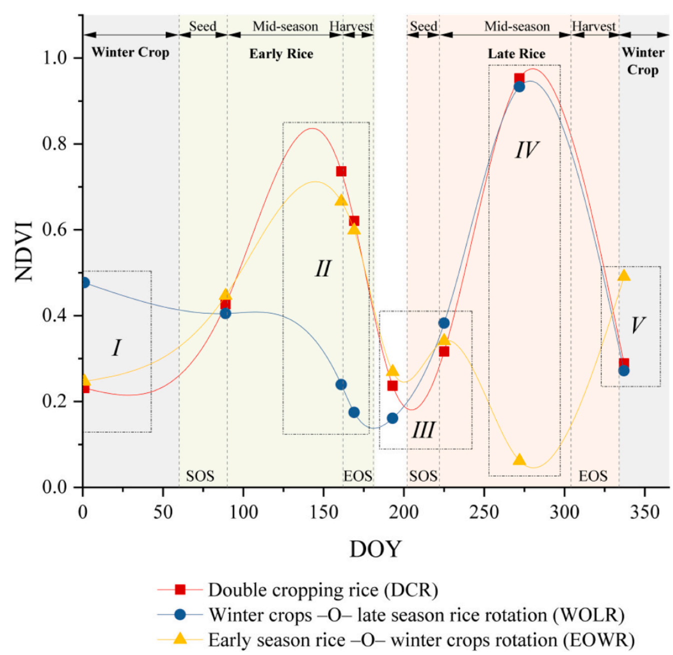

Fig. 6. NDVI profiles of the DCR, EOWR, and WOLR sequences.

4. Discussion

4.1. Advantages of the agronomic remote sensing knowledge graph for crop mapping

Crop rotations (such as the two rotations considered in our study, namely, the EOWR and WOLR sequences) increase agricultural diversity and significantly affect the organic matter content in farmland, thereby increasing the positive externalities (social, economic and ecological benefits) of rice production, as reported by He et al. (2021) and Zhu et al.

Table 4
Assessment of the accuracy of the pixel-based classification results.

Groups		Control	Exp. 1	Exp. 2	Exp. 3	Exp. 4	Exp. 5
Double-cropping rice	**PA (%)**	96.55	89.66	92.24	95.69	94.83	96.55
	UA (%)	94.12	83.87	89.17	92.50	88.71	94.12
Early-season rice–O–winter crop rotation	**PA (%)**	88.14	86.44	83.05	88.14	84.75	91.53
	UA (%)	96.30	86.44	87.50	94.55	87.72	91.53
Winter crops–O–late-season rice rotation	**PA (%)**	91.84	69.39	79.59	83.67	73.47	85.71
	UA (%)	95.74	91.89	97.50	95.35	94.74	97.67
Others	**PA (%)**	90.83	81.65	88.07	88.07	83.49	88.07
	UA (%)	88.39	80.18	83.48	84.21	81.25	86.49
OA (%)		92.49	83.48	87.39	90.09	86.19	91.29
Kappa		0.895	0.769	0.823	0.861	0.806	0.878

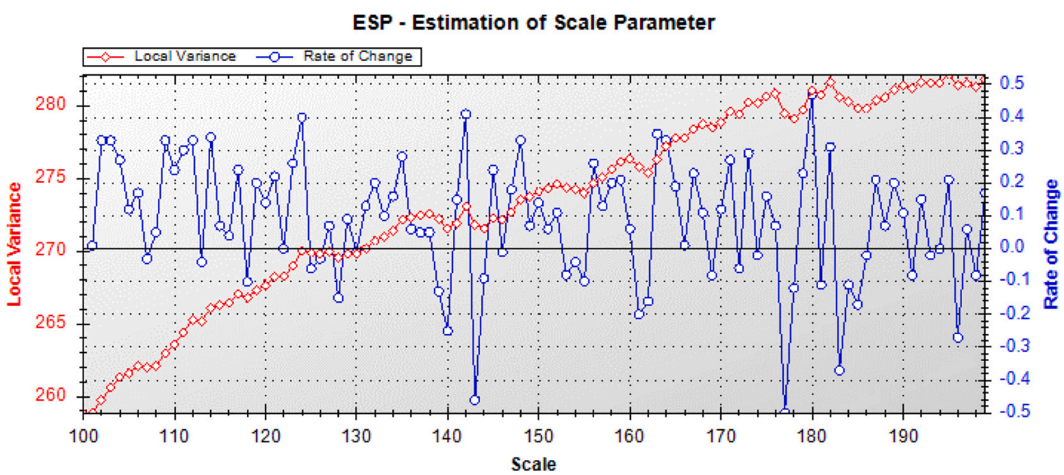

Fig. 7. Determination of the optimal scaling parameters via the ESP-2 tool.

Table 5
Assessment of the accuracy of the object-based classification results.

Groups		Control	Exp. 1	Exp. 2	Exp. 3	Exp. 4	Exp. 5
Double-cropping rice	PA (%)	97.41	95.67	93.10	97.41	94.83	94.83
	UA (%)	90.40	82.22	90.00	88.28	94.83	94.83
Early-season rice–O–winter crop rotation	PA (%)	88.14	81.36	86.44	89.83	88.14	88.14
	UA (%)	91.23	96.00	96.23	91.38	98.11	94.55
Winter crops–O–late-season rice rotation	PA (%)	97.96	57.14	83.67	97.96	61.22	83.67
	UA (%)	96.00	90.32	93.18	96.00	90.90	93.18
Others	PA (%)	88.07	88.07	89.90	85.32	94.50	93.58
	UA (%)	95.05	82.05	84.48	95.88	78.63	86.44
OA (%)		92.80	84.98	89.49	92.20	88.59	91.60
Kappa		0.900	0.787	0.853	0.891	0.839	0.882

(2022). Our approach combined crop rotation identification with knowledge graphs, which differs from previous studies that integrated different dates (Conrad et al., 2014; Luo et al., 2023; Murakami et al., 2001; Zhang et al., 2020a). We emphasized agronomic knowledge of crop sowing and phenological knowledge for crop rotation identification from the mechanism of crop growth and development. Our study enables regulatory agencies and other farm stakeholders to optimize agroecosystems for sustainable rice production.

Our theoretical framework is an improvement that refines the existing crop classification perspectives and approaches. In our study of agronomic remote sensing knowledge graphs, we proposed that key phenology events should be prioritized in selecting time windows for classification by integrating agronomic and phenological knowledge. Specifically, knowledge graphs could facilitate the monitoring of different cropping sequences and crop rotations throughout the entire growing season, including the rainy season (divided into first and second halves) and the dry season. Five key phenological events, namely, the winter crop planting period (*I*), early-season rice maturation period (*II*), early-season rice harvesting period (*III*), late-season rice maturation period (*IV*), and winter crop planting period (*V*), were subsequently identified in the study area. Image features *I* and *II* could distinguish the WOLR sequence from the DCR and EOWR sequences, whereas image features *IV* and *V* could distinguish the EOWR sequence from the DCR and WOLR sequences. For example, if data were available for only two time windows, greater accuracy could be achieved with features *II* and *IV*, as indicated by the cropping sequence mapping results of Exp. 1. Only the use of remote sensing-derived features covering two time windows (*II* and *IV*) could provide high accuracy, with the OA value exceeding 83.48 % (pixel-based) and 84.98 % (object-based).

Our theoretical framework can produce object-based crop mapping results with better accuracy. In the agronomic remote sensing knowledge graph framework, the object-based classification approach also assisted in increasing the accuracy (Wang et al., 2022). The OA value of object-based classification also showed a similar trend to that of pixel-based classification in that the OA value increased with increasing amount of remote sensing data covering more key phenology events.

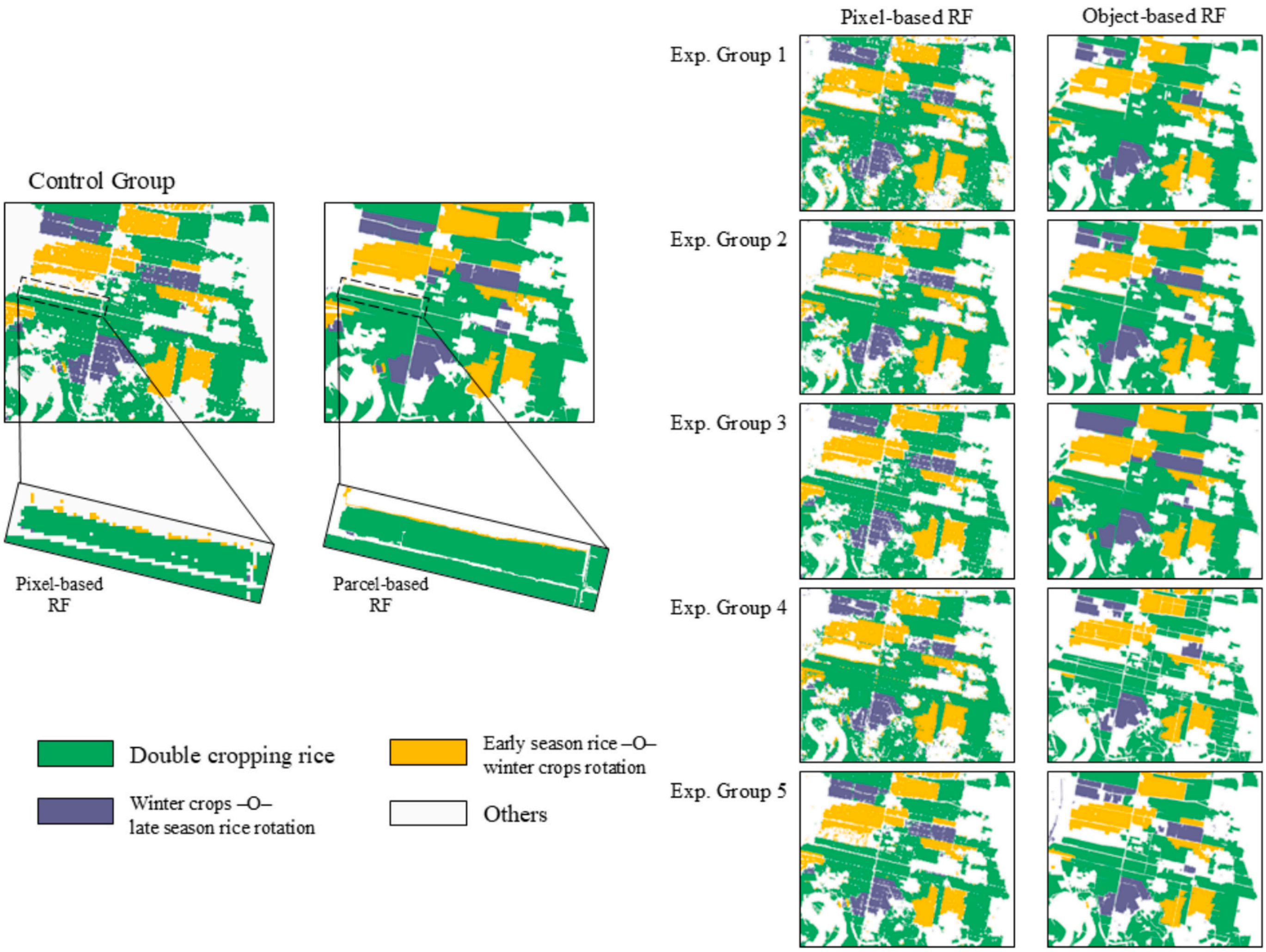

Fig. 8. Pixel- and object-based cropping sequence classification results: All groups exhibited consistent classification results, among which the control group demonstrated the best spatial detail, and object-based classification provided finer spatial detail than pixel-based classification did.

Table 6
Areal statistics of the cropping sequence classification results. (pixel-based/object-based, in km^2).

Groups	Control	Exp. 1	Exp. 2	Exp. 3	Exp. 4	Exp. 5
Double-cropping rice	15.82 / 16.97	17.16 / 17.69	16.30 / 16.55	15.63 / 17.71	16.79 / 15.09	15.43 / 15.41
Early-season rice–O–winter crop rotation	5.42 / 5.69	5.95 / 4.97	5.58 / 5.16	5.38 / 5.84	5.47 / 4.85	5.65 / 5.31
Winter crops–O–late-season rice rotation	2.97 / 3.53	2.85 / 2.04	2.78 / 2.83	2.82 / 3.63	2.78 / 2.03	2.87 / 2.91
Others	17.72 / 15.75	15.98 / 17.44	17.28 / 17.60	18.11 / 14.78	16.91 / 20.17	17.99 / 18.31

Similar to the results reported by Gao and Mas (2008), the OA value of the object-based classification results was higher than that of the pixel-based classification results. Hence, object-based classification can support accurate object identification and crop mapping.

Our theoretical framework can be employed for integrating the temporal features of crop growth and the spatial features of objects. Notably, spectral and temporal features derived from dense time series Landsat and Sentinel images can provide temporal dynamics of the spectral information of crops during the growing season to capture the crop growth process accurately. Moreover, spatial features generated from GF images can provide high-spatial-resolution information to accurately delineate the boundaries of cropland objects. Thus, in the agronomic remote sensing knowledge graph framework, we fused spatial–temporal–spectral features from those two types of remote sensing data to capitalize on their respective strengths. Similarly, Sun et al. (2023) extracted cropland objects from very high-resolution Google images (a spatial resolution of 0.55 m) and then associated them with temporal–spectral features from Sentinel-2A, Landsat-8, and GF-6 images to precisely map crop planting structures in the Yellow River Basin of Ningxia, China, thereby achieving an OA value of 80 %. Overall, fusing spatial–temporal–spectral features from multisource remote sensing data is an efficient approach for distinguishing different cropping sequences.

In addition, the results showed that some segmented objects which belong to the "Others" class using the object-based classification method were misclassified into the WOLR class, and some objects which belong to the DCR class were misclassified into the "Others" class (Fig. 8). The possible uncertainties could be triggered by three aspects: (1) a strategy of automatically and randomly selecting training and validation samples was used in this study, resulting in fewer training and validation samples being selected for some land use categories, for example, the lack of road samples which belongs to the “Others” class using this sample-selection strategy (please see, Fig. 1); (2) when the segmented object is used as the smallest classification unit, the objects of the “Others” class contain different pixels (i.e., urban, road, natural vegetation and water body) and their NDVI values are derived from the mean value of the remote sensing based pixels contained in the corresponding objects data at different key phenological events, resulting in the non-homogeneity and impurity within objects of the “Others” class and then weakening or interference of certain key features; (3) only based on those training and validation samples, the time-series remote sensing generated NDVI features at the different phenological events selected for some experimental groups also could not cover the key differentiated spectral and temporal features of various categories, resulting in the time-series NDVI not being used as a valid diagnostic indicator to accurately distinguish the “Others” class from rice cropping sequences using the object-based RF classifier. However, in the Control Group, the averaged time-series NDVI of these objects covering sufficient remote sensing data at all key events resolved this problem and captured higher classification accuracy compared to the result using the pixel-based classification method. The synergies and trade-offs between the accuracy and performance of machine learning classification based on object-oriented strategies mentioned above also disprove the necessity of our proposed mapping framework. This framework guides us to incorporate agronomic knowledge graphs integrating phenology and remote sensing into a machine learning approach to guide feature selection and cropping sequence mapping.

The simple and reliable theoretical framework proposed in this study focuses on filtering images of key phenological events, which is highly critical for utilizing limited remote sensing images to map historical cropping distributions. The proposed theoretical framework also makes it possible to accurately identify spatial-temporal variations of crops and then identify the high-quality farmland, helping geographers and agronomists to assess the suitability of crop cultivation and guiding the policymaking to maximize eco-efficiency and human well-being.

4.2. Limitations and future work

Our study highlights the importance of establishing agronomic remote sensing knowledge graphs for cropping sequence identification. By obtaining information on the spatial and temporal disturbances of agricultural natural resources driven by different management patterns and policies, we constructed and analyzed agronomic remote sensing knowledge graphs, which solved the problem of integrating spatiotemporal disturbance information into accurate management and decision-making processes. However, the dates of key rice phenological events in this study were determined via prior agronomic knowledge. Climate change and agronomic practices have altered rice phenology in recent years (Chen et al., 2021); thus, regional and temporal differences in rice cropping should be considered when adopting the methodology proposed in this study. In particular, multiyear mapping of rice cropping sequences requires yearly identification of phenological events. In addition, although object-based classification alleviated the salt-and-pepper effect and increased the accuracy, misclassification still occurred at the edges of some objects, thus increasing the uncertainty in the results. This problem could be attributed to the mixed-pixel effect due to the limited spatiotemporal resolution of the images (Chen et al., 2018).

In future research on classification algorithms, images from different types of sensors and ontologies might increase the effectiveness of knowledge graphs. The mining of semantic and contextual information may enhance the ability of knowledge graphs to accurately provide the yearly phenology of rice in different agricultural regions. For the classification algorithm, deep learning (Rawat et al., 2021) and other artificial intelligence methods should be introduced to identify cropping sequences. Moreover, the integration of synthetic aperture radar (SAR) images and optical images may increase the accuracy of the mapping results. Although NDVI profiles capture the overall temporal features of specific cropping sequences, the land surface water index (LSWI) can capture the unique properties of paddy parcels when paddy rice is transplanted in compound water–soil surface environments, thus increasing the classification accuracy (Jeong et al., 2024; Pan et al., 2018). Additionally, incorporating knowledge graphs into land suitability analysis extends the scope of application, addressing questions such as “where”, “why” and “when” in agroecology (Mugiyo et al., 2021) and improving future planning on the basis of crop production guidelines and agroecosystem management.

5. Conclusions

The tropical monsoon zone is an important source area for rice, but frequent cloud cover during the rainy season leads to insufficient availability of optical remote sensing images covering the growth stages of rice, which renders remote sensing-derived identification of rice difficult. In this work, on the basis of agronomic remote sensing knowledge graphs, we constructed a control group and five experimental groups integrating remote sensing bands and NDVI features and applied pixel- and object-based RF algorithms. The results revealed that the five key phenological events are the winter crop planting period, early-season rice maturation period, early-season rice harvesting period, late-season rice maturation period, and winter crop planting period. For both the pixel- and object-based classification results, the OA value increased since the remote sensing data covered more key phenology events. Phenology events, including the early-season rice maturation period and the late-season rice maturation period, were prioritized in cropping sequence mapping. Only with the use of features of images acquired within these two time windows could a high OA value of more than 83.48 % (pixel-based) or 84.98 % (object-based) be obtained. In addition, the object-based classification results exhibited higher OA values and finer spatial details. These findings indicate that geographical knowledge graphs coupled with remote sensing features and the rice crop phenology, growth process and state can theoretically be employed to better understand rice mapping. For efficient rice cultivation mapping via optical remote sensing data, specific time windows corresponding to phenological events must be selected. The proposed strategy facilitates the effective monitoring of rice cropping sequences, providing further evidence of planning structures for crop cultivation and thus ensuring regional food security. However, the limitations of this study should be noted. In particular, multiyear mapping of rice cropping sequences in different regions requires adaptation to local conditions. Future work should focus on improving agronomic remote sensing methods for identifying cropping sequences and enhancing agroecosystem management in tropical monsoon zones.

CRediT authorship contribution statement

Hongzhang Nie: Writing – review & editing, Writing – original draft, Validation, Software, Methodology, Formal analysis, Data curation. **Yingchen Lin:** Writing – review & editing, Validation, Formal analysis, Data curation. **Wenfei Luo:** Writing – review & editing, Validation. **Guilin Liu:** Writing – review & editing, Writing – original draft, Validation, Supervision, Project administration, Funding acquisition, Conceptualization.

Declaration of competing interest

The authors declared no potential conflicts of interest with respect to the research, authorship, and/or publication of this article.

Acknowledgments

This research was supported by Guangdong Basic and Applied Basic Research Foundation (Grant number. 2023A1515010736). We are grateful to USGS and ESA for providing Landsat and Sentinel remote sensing images and Guangdong High-resolution Earth Observation System Guangdong Data and Application Center for sharing Gaofen (GF) remote sensing images. We are sincerely grateful to the editors and anonymous reviewers for their careful comments and constructive suggestions. We also thank Bojin Huang, from Guangdong Polytechnic Normal University, for providing local cropping information.

Appendix A. Supplementary data

Supplementary data to this article can be found online at https://doi.org/10.1016/j.ecoinf.2025.103075.

Data availability

The data generated in the study are available for download from the link (https://drive.google.com/drive/folders/13_vPbKNV_DnUjBKTrWpktlN3Bx85BFzD?usp=sharing).

References

Araya, S., Ostendorf, B., Lyle, G., Lewis, M., 2018. CropPhenology: an R package for extracting crop phenology from time series remotely sensed vegetation index imagery. Eco. Inform. 46, 45–56. https://doi.org/10.1016/j.ecoinf.2018.05.006.

Avci, C., Budak, M., Yağmur, N., Balçik, F., 2023. Comparison between random forest and support vector machine algorithms for LULC classification. Int. J. Engin. Geosci. 8 (1), 1–10. https://doi.org/10.26833/ijeg.987605.

Belgiu, M., Csillik, O., 2018. Sentinel-2 cropland mapping using pixel-based and object-based time-weighted dynamic time warping analysis. Remote Sens. Environ. 204, 509–523. https://doi.org/10.1016/j.rse.2017.10.005.

Blickensdörfer, L., Schwieder, M., Pflugmacher, D., Nendel, C., Erasmi, S., Hostert, P., 2022. Mapping of crop types and crop sequences with combined time series of Sentinel-1, Sentinel-2 and Landsat 8 data for Germany. Remote Sens. Environ. 269, 112831. https://doi.org/10.1016/j.rse.2021.112831.

Breiman, L., 2001. Random forests. Mach. Learn. 45 (1), 5–32. https://doi.org/10.1023/A:1010933404324.

Caparros-Santiago, J.A., Quesada-Ruiz, L.C., Rodriguez-Galiano, V., 2023. Can land surface phenology from Sentinel-2 time-series be used as an indicator of Macaronesian ecosystem dynamics? Eco. Inform. 77, 102239. https://doi.org/10.1016/j.ecoinf.2023.102239.

Chen, W., Liu, G., 2024. A novel method for identifying crops in parcels constrained by environmental factors through the integration of a Gaofen-2 high-resolution remote sensing image and Sentinel-2 time series. IEEE J. Sel. Top. Appl. Earth Obs. Remote Sens. 17, 450–463. https://doi.org/10.1109/JSTARS.2023.3329987.

Chen, B., Huang, B., Xu, B., 2015. Comparison of spatiotemporal fusion models: a review. Remote Sens. 7 (2), 1798–1835. https://doi.org/10.3390/rs70201798.

Chen, X., Wang, D., Chen, J., Wang, C., Shen, M., 2018. The mixed pixel effect in land surface phenology: a simulation study. Remote Sens. Environ. 211, 338–344. https://doi.org/10.1016/j.rse.2018.04.030.

Chen, J., Liu, Y., Zhou, W., Zhang, J., Pan, T., 2021. Effects of climate change and crop management on changes in rice phenology in China from 1981 to 2010. J. Sci. Food Agric. 101 (15), 6311–6319. https://doi.org/10.1002/jsfa.11300.

Congalton, R.G., 1991. A review of assessing the accuracy of classifications of remotely sensed data. Remote Sens. Environ. 37 (1), 35–46. https://doi.org/10.1016/0034-4257(91)90048-B.

Conrad, C., Dech, S., Dubovyk, O., Fritsch, S., Klein, D., Löw, F., Schorcht, G., Zeidler, J., 2014. Derivation of temporal windows for accurate crop discrimination in heterogeneous croplands of Uzbekistan using multitemporal RapidEye images. Comput. Electron. Agric. 103, 63–74. https://doi.org/10.1016/j.compag.2014.02.003.

de Azevedo, R.P., Dallacort, R., Boechat, C.L., Teodoro, P.E., Teodoro, L.P.R., Rossi, F.S., Filho, W.L.F.C., Della-Silva, J.L., Baio, F.H.R., Lima, M., Silva Junior, C.A.D., 2023. Remotely sensed imagery and machine learning for mapping of sesame crop in the Brazilian Midwest. Remote Sens. Applicat.: Soc. Environ. 32, 101018. https://doi.org/10.1016/j.rsase.2023.101018.

de Beurs, K.M., Henebry, G.M., 2010. Spatio-temporal statistical methods for modelling land surface phenology. In: Hudson, I.L., Keatley, M.R. (Eds.), Phenological Research. Springer, Netherlands, pp. 177–208. https://doi.org/10.1007/978-90-481-3335-2_9.

Drăguţ, L., Tiede, D., Levick, S.R., 2010. ESP: a tool to estimate scale parameter for multiresolution image segmentation of remotely sensed data. Int. J. Geogr. Inf. Sci. 24 (6), 859–871. https://doi.org/10.1080/13658810903174803.

Drăguţ, L., Csillik, O., Eisank, C., Tiede, D., 2014. Automated parameterisation for multi-scale image segmentation on multiple layers. ISPRS J. Photogramm. Remote Sens. 88, 119–127. https://doi.org/10.1016/j.isprsjprs.2013.11.018.

Duarte, L., Teodoro, A.C., Gonçalves, H., 2014. In: Michel, U., Schulz, K. (Eds.), Deriving phenological metrics from NDVI through an open source tool developed in QGIS, p. 924511. https://doi.org/10.1117/12.2066136.

Ferchichi, A., Abbes, A.B., Barra, V., Farah, I.R., 2022. Forecasting vegetation indices from spatio-temporal remotely sensed data using deep learning-based approaches: a systematic literature review. Eco. Inform. 68, 101552. https://doi.org/10.1016/j.ecoinf.2022.101552.

Fu, Y., Shen, R., Song, C., Dong, J., Han, W., Ye, T., Yuan, W., 2023. Exploring the effects of training samples on the accuracy of crop mapping with machine learning algorithm. Sci. Remote Sens. 7, 100081. https://doi.org/10.1016/j.srs.2023.100081.

Gao, Y., Mas, J.F., 2008. A comparison of the performance of pixel-based and object-based classifications over images with various spatial resolutions. Online J. Earth Sci. 2 (1), 27–35.

Gao, F., Masek, J., Schwaller, M., Hall, F., 2006. On the blending of the Landsat and MODIS surface reflectance: predicting daily Landsat surface reflectance. IEEE Trans. Geosci. Remote Sens. 44 (8), 2207–2218. https://doi.org/10.1109/TGRS.2006.872081.

Gorelick, N., Hancher, M., Dixon, M., Ilyushchenko, S., Thau, D., Moore, R., 2017. Google Earth Engine: planetary-scale geospatial analysis for everyone. Remote Sens. Environ. 202, 18–27. https://doi.org/10.1016/j.rse.2017.06.031.

He, D.-C., Ma, Y.-L., Li, Z.-Z., Zhong, C.-S., Cheng, Z.-B., Zhan, J., 2021. Crop rotation enhances agricultural sustainability: from an empirical evaluation of eco-economic benefits in rice production. Agriculture 11 (2), 91. https://doi.org/10.3390/agriculture11020091.

Hu, Q., Wu, W., Song, Q., Lu, M., Chen, D., Yu, Q., Tang, H., 2017. How do temporal and spectral features matter in crop classification in Heilongjiang Province, China? J. Integr. Agric. 16 (2), 324–336. https://doi.org/10.1016/S2095-3119(15)61321-1.

Hughes, G., 1968. On the mean accuracy of statistical pattern recognizers. IEEE Trans. Inf. Theory 14 (1), 55–63. https://doi.org/10.1109/TIT.1968.1054102.

Jeong, S., Ko, J., Ban, J., Shin, T., Yeom, J., 2024. Deep learning-enhanced remote sensing-integrated crop modeling for rice yield prediction. Eco. Inform. 84, 102886. https://doi.org/10.1016/j.ecoinf.2024.102886.

Jiang, R., Sanchez-Azofeifa, A., Laakso, K., Xu, Y., Zhou, Z., Luo, X., Huang, J., Chen, X., Zang, Y., 2021. Cloud cover throughout all the paddy rice fields in Guangdong, China: impacts on Sentinel 2 MSI and Landsat 8 OLI optical observations. Remote Sens. 13 (15), 2961. https://doi.org/10.3390/rs13152961.

Jiao, S., Hu, D., Shen, Z., Wang, H., Dong, W., Guo, Y., Li, S., Lei, Y., Kou, W., Wang, J., He, H., Fang, Y., 2022. Parcel-level mapping of horticultural crop orchards in complex mountain areas using VHR and time-series images. Remote Sens. 14 (9), 2015. https://doi.org/10.3390/rs14092015.

Jombo, S., Adelabu, S., 2023. Evaluating Landsat-8, Landsat-9 and Sentinel-2 imageries in land use and land cover (LULC) classification in a heterogeneous urban area. GeoJournal 88 (S1), 377–399. https://doi.org/10.1007/s10708-023-10982-8.

Kang, Y., Chen, Z., Li, L., Zhang, Q., 2023. Construction of multidimensional features to identify tea plantations using multisource remote sensing data: a case study of Hangzhou city, China. Eco. Inform. 77, 102185. https://doi.org/10.1016/j.ecoinf.2023.102185.

Kuenzer, C., Knauer, K., 2013. Remote sensing of rice crop areas. Int. J. Remote Sens. 34 (6), 2101–2139. https://doi.org/10.1080/01431161.2012.738946.

Laborde, H., Douzal, V., Ruiz Piña, H.A., Morand, S., Cornu, J.-F., 2017. Landsat-8 cloud-free observations in wet tropical areas: a case study in South East Asia. Remote Sens. Lett. 8 (6), 537–546. https://doi.org/10.1080/2150704X.2017.1297543.

Leteinturier, B., Herman, J.L., Longueville, F.D., Quintin, L., Oger, R., 2006. Adaptation of a crop sequence indicator based on a land parcel management system. Agric. Ecosyst. Environ. 112 (4), 324–334. https://doi.org/10.1016/j.agee.2005.07.011.

Li, P., Jiang, L., Feng, Z., Sheldon, S., Xiao, X., & others. (2016). Mapping rice cropping systems using Landsat-derived renormalized index of normalized difference vegetation index (RNDVI) in the Poyang Lake Region, China, Front. Earth Sci., 10(2), 303–314.

Li, R., Xu, M., Chen, Z., Gao, B., Cai, J., Shen, F., He, X., Zhuang, Y., Chen, D., 2021a. Phenology-based classification of crop species and rotation types using fused MODIS and Landsat data: the comparison of a random-forest-based model and a decision-rule-based model. Soil Tillage Res. 206, 104838. https://doi.org/10.1016/j.still.2020.104838.

Li, Q., Liu, G., Chen, W., 2021b. Toward a simple and generic approach for identifying multi-year cotton cropping patterns using Landsat and Sentinel-2 time series. Remote Sens. 13 (24), 5183. https://doi.org/10.3390/rs13245183.

Liepa, A., Thiel, M., Taubenböck, H., Steffan-Dewenter, I., Abu, I.-O., Singh Dhillon, M., Otte, I., Otim, M.H., Lutaakome, M., Meinhof, D., Martin, E.A., Ullmann, T., 2024. Harmonized NDVI time-series from Landsat and Sentinel-2 reveal phenological patterns of diverse, small-scale cropping systems in East Africa. Remote Sens. Applicat.: Soc. Environ. 35, 101230. https://doi.org/10.1016/j.rsase.2024.101230.

Liu, Y., Xiao, D., Yang, W., 2022. An algorithm for early rice area mapping from satellite remote sensing data in Southwestern Guangdong in China based on feature optimization and random forest. Eco. Inform. 72, 101853. https://doi.org/10.1016/j.ecoinf.2022.101853.

Luo, K., Lu, L., Xie, Y., Chen, F., Yin, F., Li, Q., 2023. Crop type mapping in the central part of the North China Plain using Sentinel-2 time series and machine learning. Comput. Electron. Agric. 205, 107577. https://doi.org/10.1016/j.compag.2022.107577.

Mahlayeye, M., Darvishzadeh, R., Nelson, A., 2024. Characterising maize and intercropped maize spectral signatures for cropping pattern classification. Int. J. Appl. Earth Obs. Geoinf. 128, 103699. https://doi.org/10.1016/j.jag.2024.103699.

Meng, J., Xu, J., You, X., 2015. Optimizing soybean harvest date using HJ-1 satellite imagery. Precis. Agric. 16 (2), 164–179. https://doi.org/10.1007/s11119-014-9368-3.

Meng, Y., Yuan, W., Aktilek, E.U., Zhong, Z., Wang, Y., Gao, R., Su, Z., 2023. Fine hyperspectral classification of rice varieties based on self-attention mechanism. Eco. Inform. 75, 102035. https://doi.org/10.1016/j.ecoinf.2023.102035.

Mosleh, M., Hassan, Q., Chowdhury, E., 2015. Application of remote sensors in mapping rice area and forecasting its production: a review. Sensors 15 (1), 769–791. https://doi.org/10.3390/s150100769.

Mugiyo, H., Chimonyo, V.G.P., Sibanda, M., Kunz, R., Masemola, C.R., Modi, A.T., Mabhaudhi, T., 2021. Evaluation of land suitability methods with reference to neglected and underutilised crop species: a scoping review. Land 10 (2), 125. https://doi.org/10.3390/land10020125.

Murakami, T., Ogawa, S., Ishitsuka, N., Kumagai, K., Saito, G., 2001. Crop discrimination with multitemporal SPOT/HRV data in the Saga Plains, Japan. Int. J. Remote Sens. 22 (7), 1335–1348. https://doi.org/10.1080/01431160151144378.

Ni, R., Tian, J., Li, X., Yin, D., Li, J., Gong, H., Zhang, J., Zhu, L., Wu, D., 2021. An enhanced pixel-based phenological feature for accurate paddy rice mapping with Sentinel-2 imagery in Google Earth Engine. ISPRS J. Photogramm. Remote Sens. 178, 282–296. https://doi.org/10.1016/j.isprsjprs.2021.06.018.

Pan, T., Zhang, C., Kuang, W., De Maeyer, P., Kurban, A., Hamdi, R., Du, G., 2018. Time tracking of different cropping patterns using Landsat images under different agricultural systems during 1990–2050 in Cold China. Remote Sens. 10 (12), 2011. https://doi.org/10.3390/rs10122011.

Pelletier, C., Valero, S., Inglada, J., Champion, N., Dedieu, G., 2016. Assessing the robustness of random forests to map land cover with high resolution satellite image time series over large areas. Remote Sens. Environ. 187, 156–168. https://doi.org/10.1016/j.rse.2016.10.010.

Pluto-Kossakowska, J., 2021. Review on multitemporal classification methods of satellite images for crop and arable land recognition. Agriculture 11 (10), 999. https://doi.org/10.3390/agriculture11100999.

Rahmati, A., Zoej, M.J.V., Dehkordi, A.T., 2022. Early identification of crop types using Sentinel-2 satellite images and an incremental multi-feature ensemble method (case study: Shahriar, Iran). Adv. Space Res. 70 (4), 907–922. https://doi.org/10.1016/j.asr.2022.05.038.

Rawat, A., Kumar, A., Upadhyay, P., Kumar, S., 2021. Deep learning-based models for temporal satellite data processing: classification of paddy transplanted fields. Eco. Inform. 61, 101214. https://doi.org/10.1016/j.ecoinf.2021.101214.

Reed, B.C., Brown, J.F., VanderZee, D., Loveland, T.R., Merchant, J.W., Ohlen, D.O., 1994. Measuring phenological variability from satellite imagery. J. Veg. Sci. 5 (5), 703–714. https://doi.org/10.2307/3235884.

Rojo, J., Romero-Morte, J., Lara, B., Quirós, E., Richardson, A.D., Pérez-Badia, R., 2022. Biological-based and remote sensing techniques to link vegetative and reproductive development and assess pollen emission in Mediterranean grasses. Eco. Inform. 72, 101898. https://doi.org/10.1016/j.ecoinf.2022.101898.

Sah, S., Haldar, D., Chandra, S., Nain, A.S., 2023. Discrimination and monitoring of rice cultural types using dense time series of Sentinel-1 SAR data. Eco. Inform. 76, 102136. https://doi.org/10.1016/j.ecoinf.2023.102136.

Shang, R., Zhu, Z., Zhang, J., Qiu, S., Yang, Z., Li, T., Yang, X., 2022. Near-real-time monitoring of land disturbance with harmonized Landsats 7–8 and Sentinel-2 data. Remote Sens. Environ. 278, 113073. https://doi.org/10.1016/j.rse.2022.113073.

Shi, S., Zhou, S., Lei, Y., Harrison, M.T., Liu, K., Chen, F., Yin, X., 2024. Burgeoning food demand outpaces sustainable water supply in China. Agric. Water Manag. 301, 108936. https://doi.org/10.1016/j.agwat.2024.108936.

Singha, M., Sarmah, S., 2019. Incorporating crop phenological trajectory and texture for paddy rice detection with time series MODIS, HJ-1A and ALOS PALSAR imagery. Eur. J. Remote Sens. 52 (1), 73–87. https://doi.org/10.1080/22797254.2018.1556568.

Steinmann, H.-H., Dobers, E.S., 2013. Spatio-temporal analysis of crop rotations and crop sequence patterns in Northern Germany: potential implications on plant health and crop protection. J. Plant Diseas. Protect. 120 (2), 85–94. https://doi.org/10.1007/BF03356458.

Sun, Y., Yao, N., Luo, J., Leng, P., Liu, X., 2023. A spatiotemporal collaborative approach for precise crop planting structure mapping based on multi-source remote-sensing data. Int. J. Remote Sens. 1–17. https://doi.org/10.1080/01431161.2023.2217985.

Trimble Germany GmbH, 2014. Trimble Documentation eCognition Developer 9.0 User Guide. Trimble Germany GmbH.

van der Linden, S., Rabe, A., Held, M., Jakimow, B., Leitão, P., Okujeni, A., Schwieder, M., Suess, S., Hostert, P., 2015. The EnMAP-box—A toolbox and application programming interface for EnMAP data processing. Remote Sens. 7 (9), 11249–11266. https://doi.org/10.3390/rs70911249.

Wang, Y., Fang, S., Zhao, L., Huang, X., Jiang, X., 2022. Parcel-based summer maize mapping and phenology estimation combined using Sentinel-2 and time series Sentinel-1 data. Int. J. Appl. Earth Obs. Geoinf. 108, 102720. https://doi.org/10.1016/j.jag.2022.102720.

Wardlow, B.D., Egbert, S.L., 2008. Large-area crop mapping using time-series MODIS 250 m NDVI data: an assessment for the U.S. Central Great Plains. Remote Sens. Environ. 112 (3), 1096–1116. https://doi.org/10.1016/j.rse.2007.07.019.

Wu, M., Huang, W., Niu, Z., Wang, Y., Wang, C., Li, W., Hao, P., Yu, B., 2017. Fine crop mapping by combining high spectral and high spatial resolution remote sensing data in complex heterogeneous areas. Comput. Electron. Agric. 139, 1–9. https://doi.org/10.1016/j.compag.2017.05.003.

Wu, X., Xiao, X., Steiner, J., Yang, Z., Qin, Y., Wang, J., 2021. Spatiotemporal changes of winter wheat planted and harvested areas, photosynthesis and grain production in the contiguous United States from 2008–2018. Remote Sens. 13 (9), 1735. https://doi.org/10.3390/rs13091735.

Yan, S., Yao, X., Zhu, D., Liu, D., Zhang, L., Yu, G., Gao, B., Yang, J., Yun, W., 2021. Large-scale crop mapping from multi-source optical satellite imageries using machine learning with discrete grids. Int. J. Appl. Earth Obs. Geoinf. 103, 102485. https://doi.org/10.1016/j.jag.2021.102485.

Yang, Y., 2018. Study on the challenges of developing regional branding of Zhangjiang's agricultural products. Eucalypt Sci. Technol. 35 (1), 44–48. https://doi.org/10.13987/j.cnki.askj.2018.01.009.

Yang, M., Guo, B., Wang, J., 2024. A novel and robust method for large-scale single-season rice mapping based on phenology and statistical data. ISPRS J. Photogramm. Remote Sens. 213, 14–32. https://doi.org/10.1016/j.isprsjprs.2024.05.019.

Zhang, M., Lin, H., 2019. Object-based rice mapping using time-series and phenological data. Adv. Space Res. 63 (1), 190–202. https://doi.org/10.1016/j.asr.2018.09.018.

Zhang, X., Friedl, M.A., Schaaf, C.B., Strahler, A.H., Hodges, J.C.F., Gao, F., Reed, B.C., Huete, A., 2003. Monitoring vegetation phenology using MODIS. Remote Sens. Environ. 84 (3), 471–475. https://doi.org/10.1016/S0034-4257(02)00135-9.

Zhang, H., Kang, J., Xu, X., Zhang, L., 2020a. Accessing the temporal and spectral features in crop type mapping using multi-temporal Sentinel-2 imagery: a case study of Yi'an county, Heilongjiang Province, China. Comput. Electron. Agric. 176, 105618. https://doi.org/10.1016/j.compag.2020.105618.

Zhang, P., Hu, S., Li, W., Zhang, C., 2020b. Parcel-level mapping of crops in a smallholder agricultural area: a case of Central China using single-temporal VHSR imagery. Comput. Electron. Agric. 175, 105581. https://doi.org/10.1016/j.compag.2020.105581.

Zhang, X., Huang, Y., Zhang, C., Ye, P., 2022. Geoscience knowledge graph (GeoKG): development, construction and challenges. Trans. GIS 26 (6), 2480–2494. https://doi.org/10.1111/tgis.12985.

Zhao, R., Li, Y., Ma, M., 2021. Mapping paddy rice with satellite remote sensing: a review. Sustainability 13 (2), 503. https://doi.org/10.3390/su13020503.

Zhao, Y., Meng, Y., Han, S., Feng, H., Yang, G., Li, Z., 2022. Should phenological information be applied to predict agronomic traits across growth stages of winter wheat? Crop J. 10 (5), 1346–1352. https://doi.org/10.1016/j.cj.2022.08.003.

Zhu, M., She, B., Huang, L., Zhang, D., Xu, H., Yang, X., 2022. Identification of soybean based on Sentinel-1/2 SAR and MSI imagery under a complex planting structure. Eco. Inform. 72, 101825. https://doi.org/10.1016/j.ecoinf.2022.101825.